Channel Estimation for UAV-based mmWave Massive MIMO Communications with Beam Squint

Evangelos Vlachos
Industrial Systems Institute
ATHENA Research Center
Patras, Greece
evlachos@athenarc.gr

Christos Mavrokefalidis and Kostas Berberidis
Dept. of Computer Engineering and Informatics
University of Patras
Patras, Greece
{maurokef, berberid}@ceid.upatras.gr

***Abstract*—The incorporation of UAVs in 5G and envisioned 6G wireless communication systems is considered for many applications and use-cases, either as part of the infrastructure, providing coverage and connectivity (e.g., during unforeseen and rare events) or as an end-user, e.g., in remote sensing, real-time monitoring and surveillance, to name a few. From the perspective of the physical layer and the involved signal processing algorithms, the transmission environment between the UAVs and the ground communication devices, along with the utilisation of massive MIMO in the mmWave spectrum, require new channel estimation algorithms to support the required physical layer functionality. In this paper, the problem of channel estimation in a multi-user, UAV-based mmWave massive MIMO system is considered in view of the so-called beam squint effect as well as the time-varying nature of the involved channels due to mobility. The proposed approach takes advantage of the low-rank channel matrix and solves a minimisation problem via ADMM, leading to a low complexity, iterative algorithm. The performance of the proposed algorithm is evaluated via simulations and its efficacy is demonstrated over other algorithms from the relevant literature.**

***Index Terms*—mmWaves, channel estimation, UAVs, ADMM, time-varying channel, beam squint, massive MIMO**

I. Introduction

In recent years, there have been increasing research efforts towards integrating Unmanned Aerial Vehicles (UAVs) into wireless communications systems [1], [2]. UAVs can be considered in various applications either as part of the system itself (e.g., for serving as access points or relays aiming at increased coverage and connectivity) or as end-users (e.g., for delivering goods, real-time monitoring, remote sensing and precision agriculture). The envisioned applications build upon unique features of UAVs like the ability to adapt their position (including, notably, their altitude), improve large-scale transmission conditions by avoiding obstacles, and rapidly deploy during unforeseen or rare events.

The key features that make UAVs attractive in the context of wireless communications, raise also a number of challenges that need to be considered. In particular, the involved channels between UAVs and ground end-devices can be quite different when compared to conventional ground wireless channels [3]. As the UAVs are able to move in the 3D space, signals could encounter significantly different, time-varying transmission conditions or produce considerable interference to ground communication devices, including multiple base stations, due to strong Line-of-Sight (LoS) signal components [4]. These challenges are even more demanding when, also, mmWave transmissions are considered for increasing throughput and reducing latency in 5G and envisioned 6G use-cases [5]. To address these challenges, the massive Multiple-Input Multiple-Output (mMIMO) technology [6], [7] has a central role in the design of effective UAV-based wireless communications systems [8]. However, mMIMO, when used to transmit signals in large bandwidths available in the mmWave spectrum, raises yet another challenge related to the so-called beam squint effect due to measurable propagation delays manifesting along the large antenna arrays [9], [10]. This challenge leads to a more elaborate channel model that requires many signal processing operations at the transceiver to be revised [11].

In order to capitilize on the full gains of mMIMO in UAVs, accurate channel state information is of paramount importance for various operations at the physical layer like beamforming [3]. Effective channel estimation and tracking techniques [11] are expected to take into account not only the specific time-varying transmission conditions with strong LoS components due to high-altitude mobility, etc., but, also, consider the effect of beam squint when the mmWave spectrum is utilized. Focusing on the relevant literature, [12] proposed a channel estimation approach with a random spatial sampling structure, leading to improved performance for short training sequences and discussed a possible extension that takes into account the beam squint effect. In [13], [14] and [15], compressive sensing-based, off-grid sparse Bayesian learning-based and block sparsity-based channel estimation algorithms, respectively, were presented for mmWave mMIMO systems, including the beam squint effect. In [16], the effect was tackled by dividing the bandwidth into subbands and employing a spatial spectrum-based channel estimation technique. Finally, [17] proposed a channel estimation algorithm for a UAV-based system, which considers not only the beam squint effect but also, in contrast to the previous works, the time varying nature of the involved channels.

In this paper, we study the problem of uplink channel estimation in a multi-user UAV-based mmWave mMIMO wireless

Funded in part by the Project IRIDA under the Cypriot Grant RIF-INFRASTRUCTURES/1216/0017 and in part by the University of Patras.

communication system similar to the one in [17]. By adopting a parametric model for the channel that captures the effects of beam squint and Doppler due to mobility, an efficient, iterative channel estimation algorithm is proposed based on the Alternating Direction Method of Multipliers (ADMM). The proposed algorithm exploits the inherent low-rank property of the multi-user channel gain matrix and does not require knowledge of the exact number of the participating users (apart from a "worst-case" upper bound), leading to a procedure of low complexity. The performance of the algorithm is evaluated via simulations and is compared favorably to other algorithms from the relevant literature.

In the following, Sec. II describes the adopted channel model and the multi-user, UAV-based wireless communication system. The problem formulation and the proposed channel estimation algorithm are presented in Sec. III. The performance evaluation of the proposed algorithm is provided in Sec. IV and, finally, Sec. V concludes the paper.

Notation: $\mathbf{A}$, $\mathbf{a}$ and a denote a matrix, a vector and a scalar, respectively. The complex conjugate transpose and transpose of $\mathbf{A}$ are denoted as $\mathbf{A}^H$ and $\mathbf{A}^{\mathrm{T}}$, respectively. $\mathbf{I}_N$ represents the $N \times N$ identity matrix. $\mathbf{X} \in \mathbb{C}^{A\times B}$, $\mathbf{X} \in \mathbb{R}^{A\times B}$, and $\mathbf{X} \in \mathbb{I}^{A\times B}$ denote the $\mathbf{X}$ matrix of size $A \times B$ with complex, real, and imaginary entries, respectively. $\mathcal{CN}(\mathbf{a}, \mathbf{A})$ denotes a complex Gaussian vector having mean $\mathbf{a}$ and covariance $\mathbf{A}$. $[\mathbf{A}]_{kl}$ is the matrix entry at the k-th row and l-th column. Finally, $\|\cdot\|_*$ and $\|\cdot\|_F$ are the nuclear and Frobenius norms, respectively, while $\otimes$ and $\odot$ denote the Kronecker and the Hadamard products, respectively.

II. System and Channel Description

The wireless system that is adopted, comprises a single UAV that employs a Uniform Linear Array (ULA) with N antenna elements and K single antenna ground devices. Moreover, it is assumed that Orthogonal Frequency Division Multiplexing (OFDM) is employed with M subcarriers. Furthermore, it is assumed that P subcarriers in each OFDM symbol are used for transmitting pilot symbols for channel estimation purposes. Let us denote the set $\mathcal{P}$ of the pilot subcarrier indexes as $\mathcal{P} = \{p_1, p_2, \ldots, p_P\}$. Finally, in the following, T_s is the symbol duration (thus, the OFDM symbol duration is $T = MT_s$), W is the bandwidth of the transmitting channel with carrier frequency f_c and wavelength λ, c is the speed of light and $d = \lambda/2$ is the spacing of adjacent antenna elements of the UAV's ULA.

Moving on with the adopted channel model, we follow the approach presented in [17] for incorporating the effect of beam squint and Doppler, while only the dominant LoS component is retained. Hence, the continuous time-frequency representation of the channel impulse response between the k-th user and the UAV can be written as the $N \times 1$ vector

$$\mathbf{h}_k(t, f) = a_k(t) e^{-j2\pi f_{d,k}(t)t} \mathbf{a}(\theta_k(t), f), \tag{1}$$

where $a_k(t)$, $\theta_k(t)$ and $f_{d,k}(t)$ are the complex channel gain, the Angle of Arrival (AoA), and the Doppler shift, respectively, while $\mathbf{a}(\theta_k(t), f)$ is the $N \times 1$ steering vector, which is frequency dependent, thus, capturing the beam squint effect. The n-th element of the vector, with $n = 0, 1, \ldots, N-1$, can be written as

$$[\mathbf{a}(\theta_k(t), f)]_n = e^{-j\frac{2\pi n d \sin\theta_k(t)}{\lambda}\left(1+\frac{f}{f_c}\right)}. \tag{2}$$

Under a block fading assumption (as, also, adopted in [17]), the parameters $a_k(t) = a_k$, $\theta_k(t) = \theta_k$ and $f_{d,k}(t) = f_{d,k}$ are considered constant for L consecutive OFDM symbols and, thus, the discrete time-frequency equivalent channel model can be written as

$$\mathbf{h}_k(l, q) \triangleq \mathbf{h}_k(lT, q\Delta f) = a_k e^{-j2\pi l f_{d,k} T} \mathbf{a}(\theta_k, q\Delta f), \tag{3}$$

where $\Delta f = W/M$ is the sub-carrier spacing and (l, q) indexes the q-th sub-channel of the l-th OFDM symbol.

Finally, before describing the input-output relation for the received signal at the UAV corresponding to the pilot subcarriers indexed by $\mathcal{P}$, the channels $\mathbf{h}_k(l, q)$, for $l = 0, \ldots, L-1$, are put together in the following $LN \times 1$ vector.

$$\mathbf{q}_k(q) = a_k \mathrm{vec}\left(\mathbf{a}(\theta_k, q\Delta f)\mathbf{b}^{\mathrm{T}}(f_{d,k})\right) = a_k \mathbf{p}_k(q; \theta_k, f_{d,k}), \tag{4}$$

where $\mathbf{b}^{\mathrm{T}}(f_{d,k}) = [1, e^{-j2\pi f_{d,k}T}, \ldots, e^{-j2\pi(L-1)f_{d,k}T}]$ and $\mathbf{p}_k(q; \theta_k, f_{d,k})$ is parameterized over θ_k and $f_{d,k}$. Assuming that each user k repeats the pilot symbols $\mathbf{x}_k = [x_{k,1}, x_{k,2}, \ldots, x_{k,P}]^{\mathrm{T}}$ in all consecutive L OFDM symbols (as in [17]), the corresponding received signal at the UAV is written as

$$\mathbf{Y} = \sum_{k=1}^{K} a_k \mathbf{H}_k(\theta_k, f_{d,k}) \mathbf{X}_k + \mathbf{W}, \tag{5}$$

where $\mathbf{H}_k(\theta_k, f_{d,k})$ is an $LN \times P$ matrix having as columns the vectors $\{\mathbf{p}_k(q; \theta_k, f_{d,k})\}$, $q \in \mathcal{P}$, and the $LN \times P$ matrix $\mathbf{W}$ captures additive noise with elements independent and identically distributed as $[\mathbf{W}]_{lk} \sim \mathcal{CN}(0, \sigma_w^2)$. Finally, $\mathbf{X}_k$ is a $P \times P$ diagonal matrix with the elements (i.e., pilot symbols) of $\mathbf{x}_k$ in its diagonal.

III. Proposed Approach

In this Section, we introduce the proposed approach for the estimation of the channel which is formed between the K single antenna ground devices and the UAV that employs a ULA with N antenna elements. In this work, we consider the parametric estimation of the channel, thus, we aim at the estimation of the channel gains vector $\boldsymbol{\alpha} \in \mathbb{C}^{K\times 1}$, the vector with the Doppler shifts $\mathbf{f}_d \in \mathbb{R}^{K\times 1}$, and the AoAs vector $\boldsymbol{\theta} \in \mathbb{R}^{K\times 1}$. First, let us rewrite the summation term in (5) as

$$\mathbf{H}_e = \bar{\mathbf{H}}\mathbf{A}, \tag{6}$$

where $\bar{\mathbf{H}} \triangleq \left[\begin{array}{ccc} \mathbf{H}_1(\theta_1, f_{d,1}) & \ldots & \mathbf{H}_K(\theta_K, f_{d,K}) \end{array}\right]$ and $\mathbf{A} \triangleq \left[\begin{array}{ccc} \alpha_1 \mathbf{X}_1^{\mathrm{T}} & \ldots & \alpha_K \mathbf{X}_K^{\mathrm{T}} \end{array}\right]^{\mathrm{T}}$. Then, $\mathbf{A} \in \mathbb{C}^{KP\times P}$ is a low-rank matrix given that the number of users is much lower than the number of subcarriers $K \ll P$. On this premise, we propose a low-rank channel estimation, where the problem is formulated as

$$\min_{\boldsymbol{\alpha}, \mathbf{f}_d, \boldsymbol{\theta}} \|\mathbf{A}\|_* \text{ subject to } \|\mathbf{Y} - \bar{\mathbf{H}}\mathbf{A}\|_F^2 \leq \kappa, \tag{7}$$

where κ is the estimation accuracy parameter which depends on the noise variance σ_w^2.

In this work, we consider the special case where $\mathbf{X}_k = \mathbf{I}_P$, thus, matrix $\mathbf{A}$ becomes $\boldsymbol{\alpha} \otimes \mathbf{I}_P$. We choose to solve (7) using ADMM, due to its convergence properties. To do so, we introduce the auxiliary variable $\boldsymbol{\beta} \in \mathbb{C}^{K\times 1}$ that will help to decompose the cost function of (7) into a sum of two separate terms, i.e.,

$$\begin{aligned} &\min_{\boldsymbol{\alpha},\mathbf{f}_d,\boldsymbol{\theta},\boldsymbol{\beta}} \tau \|(\boldsymbol{\alpha}\otimes \mathbf{I}_P)\|_* + \|\mathbf{Y} - \bar{\mathbf{H}}(\boldsymbol{\beta}\otimes\mathbf{I}_P)\|_F^2 \\ &\text{subject to } \boldsymbol{\alpha} = \boldsymbol{\beta}, \end{aligned} \tag{8}$$

where the nuclear norm is defined as $\|\mathbf{X}\|_* \triangleq \sum \sigma(\mathbf{X})$. Parameter $\tau > 0$ provides a weighting between the two terms of the cost function, i.e., the low-rank property and the reconstruction accuracy.

The augmented Lagrangian function is expressed as

$$\begin{aligned} \mathcal{L}_\rho(\boldsymbol{\alpha},\mathbf{f}_d,\boldsymbol{\theta},\boldsymbol{\beta},\mathbf{z}) =& \tau\|\boldsymbol{\alpha}\otimes\mathbf{I}_P\|_* + \|\mathbf{Y} - \bar{\mathbf{H}}(\boldsymbol{\beta}\otimes\mathbf{I}_P)\|_F^2 \\ &+ \mathbf{z}^H(\boldsymbol{\alpha}-\boldsymbol{\beta}) + \frac{\rho}{2}\|\boldsymbol{\alpha}-\boldsymbol{\beta}\|^2, \end{aligned} \tag{9}$$

where $\rho > 0$ is the dual update step length. Following the ADMM methodology, at the (ℓ)-th ADMM algorithmic iteration, with $\ell = 1, 2, \ldots$, the following separate sub-problems have to be solved:

$$\boldsymbol{\alpha}^{(\ell+1)} = arg\min_{\boldsymbol{\alpha}} \mathcal{L}_\rho(\boldsymbol{\alpha},\mathbf{f}_d^{(\ell)},\boldsymbol{\theta}^{(\ell)},\boldsymbol{\beta}^{(\ell)},\mathbf{z}^{(\ell)}) \tag{10}$$

$$\mathbf{f}_d^{(\ell+1)} = arg\min_{\mathbf{f}_d} \mathcal{L}_\rho(\boldsymbol{\alpha}^{(\ell+1)},\mathbf{f}_d,\boldsymbol{\theta}^{(\ell)},\boldsymbol{\beta}^{(\ell)},\mathbf{z}^{(\ell)}) \tag{11}$$

$$\boldsymbol{\theta}^{(\ell+1)} = arg\min_{\boldsymbol{\theta}} \mathcal{L}_\rho(\boldsymbol{\alpha}^{(\ell+1)},\mathbf{f}_d^{(\ell+1)},\boldsymbol{\theta},\boldsymbol{\beta}^{(\ell)},\mathbf{z}^{(\ell)}) \tag{12}$$

$$\boldsymbol{\beta}^{(\ell+1)} = arg\min_{\boldsymbol{\beta}} \mathcal{L}_\rho(\boldsymbol{\alpha}^{(\ell+1)},\mathbf{f}_d^{(\ell+1)},\boldsymbol{\theta}^{(\ell+1)},\boldsymbol{\beta},\mathbf{z}^{(\ell)}) \tag{13}$$

$$\mathbf{z}^{(\ell+1)} = \mathbf{z}^{(\ell)} + \rho(\boldsymbol{\alpha}^{(\ell+1)} - \boldsymbol{\beta}^{(\ell+1)}), \tag{14}$$

with $\boldsymbol{\alpha}^{(0)} = \mathbf{f}_d^{(0)} = \boldsymbol{\theta}^{(0)} = \boldsymbol{\beta}^{(0)} = \mathbf{z}^{(0)} = \mathbf{0}$.

1) Solving (10)*:* Removing from $\mathcal{L}_\rho$ the terms which are not affected by $\boldsymbol{\alpha}$, we end up with the minimization of

$$\min_{\boldsymbol{\alpha}} \tau\|\boldsymbol{\alpha}\otimes\mathbf{I}_P\|_* + (\mathbf{z}^{(\ell)})^H(\boldsymbol{\alpha}-\boldsymbol{\beta}^{(\ell)}) + \frac{\rho}{2}\|\boldsymbol{\alpha}-\boldsymbol{\beta}^{(\ell)}\|^2, \tag{15}$$

which by completing the square becomes

$$\min_{\boldsymbol{\alpha}} \tau\|\boldsymbol{\alpha}\otimes\mathbf{I}_P\|_* + \frac{\rho}{2}\|\boldsymbol{\alpha} + \frac{\sqrt{2}}{\sqrt{\rho}}\mathbf{z}^{(\ell)} - \boldsymbol{\beta}^{(\ell)}\|^2, \tag{16}$$

which is a strictly convex problem and can be solved with the Singular Value Thresholding (SVT) algorithm [18].

2) Solving (11) *and* (12)*:* To solve over $\mathbf{f}_d$, the gradient descent technique is employed for each k for a fixed step size γ and for a predefined number of iterations $i = 1, 2, \ldots, I_{\text{max}}$. Thus,

$$f_{d,k}^{(\ell,i)} = f_{d,k}^{(\ell,i-1)} - \gamma\frac{\partial\mathcal{L}_\rho}{\partial f_{d,k}}. \tag{17}$$

To obtain the partial derivatives of the scalar function $\mathcal{L}_\rho(\mathbf{f}_d)$ for each $f_{d,k}$ with $k = 1, 2, \ldots, K$, let us first write the general rule for differentiation as

$$\frac{\partial\mathcal{L}_\rho}{\partial f_{d,k}} = \text{tr}\left\{\left(\frac{\partial\mathcal{L}_\rho}{\partial\bar{\mathbf{H}}}\right)^H \frac{\partial\bar{\mathbf{H}}}{\partial f_{d,k}}\right\} \tag{18}$$

$$= -2\text{tr}\left\{(\boldsymbol{\beta}\otimes\mathbf{I}_P)(\mathbf{Y} - \bar{\mathbf{H}}(\boldsymbol{\beta}\otimes\mathbf{I}_P))^H \frac{\partial\bar{\mathbf{H}}}{\partial f_{d,k}}\right\}, \tag{19}$$

where

$$\frac{\partial\bar{\mathbf{H}}}{\partial f_{d,k}} = \mathbf{U}\odot\bar{\mathbf{H}}, \tag{20}$$

with $\mathbf{U} \in \{0,1\}^{NL\times KP}$ being an all zero matrix except for P columns which correspond to the $\mathbf{H}_k$ matrix. The n to $n+L-1$ elements of the p-th of these P non-zero columns, are given by

$$[\mathbf{u}_p]_{n:n+L-1} = -j2\pi n(1 + p\mathbf{1}_{L\times 1}), \tag{21}$$

where $n = 0, 1, \ldots, N-1$, $p = 0, 1, \ldots, P-1$, and $\mathbf{1}_{L\times 1}$ is an $L\times 1$ all units vector. Similarly, to solve over $\boldsymbol{\theta}$, a number of gradient descent steps are performed, i.e.,

$$\theta_k^{(\ell,i)} = \theta_k^{(\ell,i-1)} - \gamma\frac{\partial\mathcal{L}_\rho}{\partial\theta_k}, \tag{22}$$

where the gradient is expressed as

$$\frac{\partial\mathcal{L}_\rho}{\partial\theta_k} = -2\text{tr}\left\{(\boldsymbol{\beta}\otimes\mathbf{I}_P)(\mathbf{Y} - \bar{\mathbf{H}}(\boldsymbol{\beta}\otimes\mathbf{I}_P))^H \frac{\partial\bar{\mathbf{H}}}{\partial\theta_k}\right\}, \tag{23}$$

where the partial derivatives over θ_k for $k = 1, 2, \ldots, K$, are given by

$$\frac{\partial\bar{\mathbf{H}}}{\partial\theta_k} = \mathbf{Q}\odot\bar{\mathbf{H}}, \tag{24}$$

with $\mathbf{Q} \in \{0,1\}^{NL\times KP}$ being an all zero matrix except for P columns which correspond to the $\mathbf{H}_k$ matrix. The n to $n+N-1$ elements of the p-th of these P columns are given by

$$[\mathbf{q}_p]_{n:n+N-1} = -j2\pi l\mathbf{1}_{N\times 1}. \tag{25}$$

3) Solving (13)*:* Keeping only the terms related to $\boldsymbol{\beta}$, the ADMM sub-problem (13) becomes

$$\min_{\boldsymbol{\beta}} \|\mathbf{Y} - \bar{\mathbf{H}}(\boldsymbol{\beta}\otimes\mathbf{I}_P)\|_F^2 - (\mathbf{z}^{(\ell)})^H\boldsymbol{\beta} + \frac{\rho}{2}\|\boldsymbol{\alpha}^{(\ell+1)} - \boldsymbol{\beta}\|^2. \tag{26}$$

Using the general rule for differentiation, we have that

$$\frac{\partial\mathcal{L}}{\partial\beta_k} = \text{tr}\left\{\left(\frac{\partial\mathcal{L}}{\partial\mathbf{B}}\right)^H \frac{\partial\mathbf{B}}{\partial\beta_k}\right\} - z_k^{(\ell)} + \rho(\alpha_k^{(\ell+1)} - \beta_k) \tag{27}$$

$$= -2\text{tr}\left\{(\mathbf{Y} - \bar{\mathbf{H}}\mathbf{B})^H\bar{\mathbf{H}}\frac{\partial\mathbf{B}}{\partial\beta_k}\right\} - z_k^{(\ell)} + \rho(\alpha_k^{(\ell+1)} - \beta_k) \tag{28}$$

$$\begin{aligned} =& -2\text{tr}\left\{\mathbf{Y}\bar{\mathbf{H}}^H\frac{\partial\mathbf{B}}{\partial\beta_k}\right\} + 2\text{tr}\left\{\mathbf{B}^H\bar{\mathbf{H}}^H\bar{\mathbf{H}}\frac{\partial\mathbf{B}}{\partial\beta_k}\right\} \\ &- z_k^{(\ell)} + \rho(\alpha_k^{(\ell+1)} - \beta_k) \end{aligned} \tag{29}$$

where $\mathbf{B} \triangleq \boldsymbol{\beta}\otimes\mathbf{I}_P$, and

$$\frac{\partial\mathbf{B}}{\partial\beta_k} = \frac{\partial\boldsymbol{\beta}}{\partial\beta_k}\otimes\mathbf{I}_P + \boldsymbol{\beta}\otimes\frac{\partial\mathbf{I}_P}{\partial\beta_k} = \mathbf{e}_k\otimes\mathbf{I}_P,$$

Algorithm 1 Proposed Channel Estimation

Require: $\mathbf{Y}$, γ
Ensure: $\boldsymbol{\alpha}$, f_d, $\boldsymbol{\theta}$

```
for ℓ = 1, 2, ... do
    Use SVT algorithm to solve (16)
    for k = 1, 2, ..., K do
        for i = 1, 2, ..., I_max do
            Perform a gradient descent step (17)
            Compute the gradient (19)
        end for
    end for
    for k = 1, 2, ..., K do
        for i = 1, 2, ..., I_max do
            Perform a gradient descent step (22)
            Compute the gradient (23)
        end for
    end for
end for
Solve the problem (26)
Perform a dual variable update (14)
```

where $\mathbf{e}_k$ is a $K \times 1$ vector which has a unit element at the k-th position and zeros elsewhere. Solving $\frac{\partial \mathcal{L}}{\partial \beta_k} = 0$ provides an estimation of β_k.

Complexity: The Algorithm 1 consists of 5 ADMM steps, which have to be repeated for a number of iterations till convergence. At each ADMM iteration, the complexity of each step depends on the number of antennas N, the number of subcarriers P, the number of the stacked blocks L, and the number of the users K. Furthermore, the solutions of (11) and (12) require additional iterations due to the gradient descent technique. However, the overall complexity is governed by the complexity of the ADMM subproblem in (13). Specifically, the complexity of the multiplication of $\bar{\mathbf{H}}^H\bar{\mathbf{H}}$ is upper bounded by $\mathcal{O}(NL(KP)^2)$. This is much lower than the complexity of Algorithm 1 in [17].

IV. Simulation Results

In this Section, we evaluate the proposed technique via the Mean Square Error (MSE) of the channel parameters estimation, defined as:

$$\mathrm{MSE}_\alpha \triangleq \frac{1}{I_{\text{reals}}} \sum_{i=1}^{I_{\text{reals}}} \frac{\|\boldsymbol{\alpha} - \hat{\boldsymbol{\alpha}}\|^2}{\|\boldsymbol{\alpha}\|^2}. \tag{30}$$

The notation $\hat{\boldsymbol{a}}$ refers to the estimation of $\boldsymbol{a}$ and I_{reals} is the number of Monte-Carlo realisations.

System setup: We compare the MSE of the technique presented in [17] and the proposed Algorithm 1, for $I_{\text{reals}} = 100$. The LoS mmWave channel is simulated at $f_c = 28$ GHz with bandwidth $W = 600$ MHz, symbol duration $T_s = \frac{1}{W}$ and $M = 1024$ subcarriers. The number of pilot subcarriers is set to $P = 4$, and the number of OFDM blocks is set to $L = 12$. The antenna size for the UAV is $N = 32$ and the K devices are specified in each experiment. We assume that the UAV has maximum relative speed $v = 80$km/h with the ground devices. This results into the maximum Doppler spread

$$f_{d,\max} = \frac{v}{c} f_c \approx 2 \text{ KHz} \tag{31}$$

The parameters for the proposed algorithm are set as $\tau = 1$, $\gamma = 10^{-1}$, and $\kappa = \|\mathbf{W}\|_F^2$. The parameters for the Algorithm 1 in [17] are set as $K = K_M = 4$, $\lambda_0 = 10^{-3}$, $\lambda_{\min} = 10^{-8}$, and $\epsilon = 10^{-3}$.

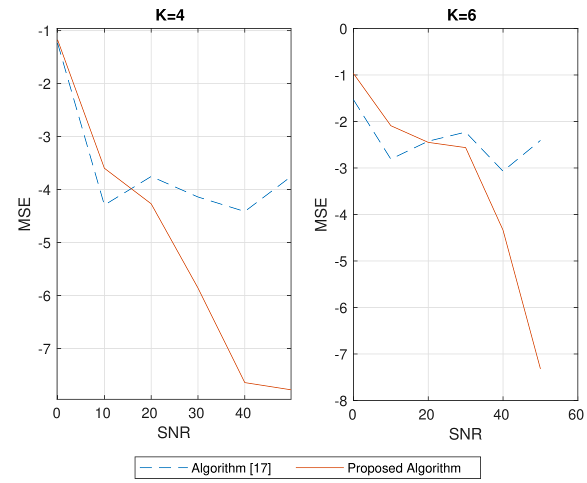

Fig. 1. Mean-square-error for the estimation of the channel gains $\boldsymbol{\alpha}$ versus the SNR, for $K = 4$ and $K = 6$.

Estimation performance: Let us first evaluate the results with respect to the Signal-to-Noise Ratio (SNR), which is defined as

$$\mathrm{SNR} \triangleq \frac{N}{\sigma_w^2}. \tag{32}$$

In Fig. 1, we provide the MSE performance of the proposed technique versus Algorithm 1 in [17]. Two cases for the number of devices are considered, namely, $K = 4$ and $K = 6$. The performance of both techniques for low and mid SNR values is limited and worsens as the number of the users K increases. This is due to the bad condition of $\mathbf{H}_e$ in (6), which is related to the orthogonality of the channels between different users. However, due to the exploitation of the low-rank property, the proposed technique exhibits much lower error floor for the higher SNR regime, in both cases.

In Fig. 2, we show the MSE results for the estimation of the channel gains $\boldsymbol{\alpha}$, over the number of users K. It is observed that, as the number of users K increases, the MSE also increases. This is expected given that the number of unknowns becomes larger and, thus, the difficulty to solve the problem. Also, similar MSE behaviour has been observed for the estimation of $\boldsymbol{\theta}$ and $\mathbf{f}_d$, over SNR and the number of users.

V. Conclusion

In this paper, the problem of channel estimation in a multi-user, UAV-based mmWave massive MIMO system is considered in view of the so-called beam squint effect as well

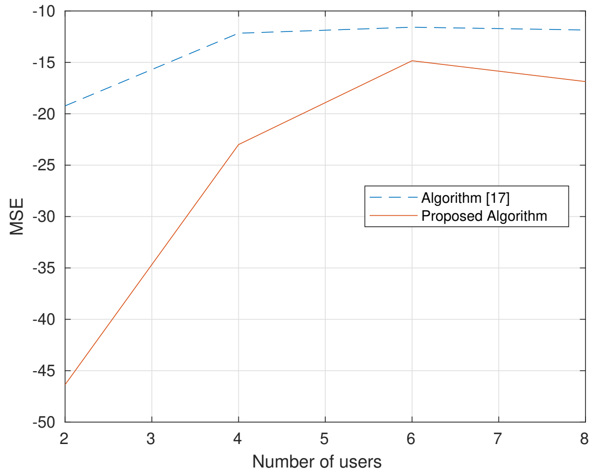

Fig. 2. Mean-square-error for the estimation of the channel gains $\boldsymbol{\alpha}$ versus the number of the users K.

as the time-varying nature of the involved channels due to mobility. The proposed algorithm exploits the inherent low-rank property of the multi-user channel gain matrix and does not require knowledge of the exact number of the participating users (apart from a "worst-case" upper bound), leading to a procedure of low complexity. This work can be extended towards some interesting directions, such as considering more general channel models that incorporate both LoS and non LoS components.

References

[1] M. Mozaffari, W. Saad, M. Bennis, Y.-H. Nam, and M. Debbah, "A tutorial on UAVs for wireless networks: Applications, challenges, and open problems," *IEEE Communications Surveys & Tutorials*, vol. 21, no. 3, pp. 2334–2360, 2019.

[2] H. Shakhatreh, A. H. Sawalmeh, A. Al-Fuqaha, Z. Dou, E. Almaita, I. Khalil, N. S. Othman, A. Khreishah, and M. Guizani, "Unmanned aerial vehicles (UAVs): A survey on civil applications and key research challenges," *IEEE Access*, vol. 7, pp. 48 572–48 634, 2019.

[3] Y. Huang, Q. Wu, R. Lu, X. Peng, and R. Zhang, "Massive MIMO for cellular-connected UAV: Challenges and promising solutions," *IEEE Communications Magazine*, vol. 59, no. 2, pp. 84–90, 2021.

[4] G. Geraci, A. Garcia-Rodriguez, L. G. Giordano, D. López-Pérez, and E. Björnson, "Understanding UAV cellular communications: From existing networks to massive MIMO," *IEEE Access*, vol. 6, pp. 67 853–67 865, 2018.

[5] Z. Xiao, L. Zhu, Y. Liu, P. Yi, R. Zhang, X.-G. Xia, and R. Schober, "A survey on millimeter-wave beamforming enabled UAV communications and networking," *IEEE Communications Surveys & Tutorials*, 2022.

[6] L. Lu, G. Y. Li, A. L. Swindlehurst, A. Ashikhmin, and R. Zhang, "An overview of massive MIMO: Benefits and challenges," *IEEE Journal of Selected Topics in Signal Processing*, vol. 8, no. 5, pp. 742–758, 2014.

[7] E. Björnson, E. G. Larsson, and T. L. Marzetta, "Massive MIMO: Ten myths and one critical question," *IEEE Communications Magazine*, vol. 54, no. 2, pp. 114–123, 2016.

[8] A. Garcia-Rodriguez, G. Geraci, D. López-Pérez, L. G. Giordano, M. Ding, and E. Bjornson, "The essential guide to realizing 5g-connected UAVs with massive MIMO," *IEEE Communications Magazine*, vol. 57, no. 12, pp. 84–90, 2019.

[9] B. Wang, F. Gao, S. Jin, H. Lin, and G. Y. Li, "Spatial-and frequency-wideband effects in millimeter-wave massive MIMO systems," *IEEE Transactions on Signal Processing*, vol. 66, no. 13, pp. 3393–3406, 2018.

[10] B. Wang, F. Gao, S. Jin, H. Lin, G. Y. Li, S. Sun, and T. S. Rappaport, "Spatial-wideband effect in massive MIMO with application in mmWave systems," *IEEE Communications Magazine*, vol. 56, no. 12, pp. 134–141, 2018.

[11] M. Wang, F. Gao, S. Jin, and H. Lin, "An overview of enhanced massive MIMO with array signal processing techniques," *IEEE Journal of Selected Topics in Signal Processing*, vol. 13, no. 5, pp. 886–901, 2019.

[12] E. Vlachos, G. C. Alexandropoulos, and J. Thompson, "Wideband mimo channel estimation for hybrid beamforming millimeter wave systems via random spatial sampling," *IEEE Journal of Selected Topics in Signal Processing*, vol. 13, no. 5, pp. 1136–1150, 2019.

[13] B. Wang, M. Jian, F. Gao, G. Y. Li, and H. Lin, "Beam squint and channel estimation for wideband mmWave massive MIMO-OFDM systems," *IEEE Transactions on Signal Processing*, vol. 67, no. 23, pp. 5893–5908, 2019.

[14] M. Jian, F. Gao, Z. Tian, S. Jin, and S. Ma, "Angle-domain aided UL/DL channel estimation for wideband mmWave massive MIMO systems with beam squint," *IEEE Transactions on Wireless Communications*, vol. 18, no. 7, pp. 3515–3527, 2019.

[15] M. Wang, F. Gao, N. Shlezinger, M. F. Flanagan, and Y. C. Eldar, "A block sparsity based estimator for mmWave massive MIMO channels with beam squint," *IEEE Transactions on Signal Processing*, vol. 68, pp. 49–64, 2020.

[16] H. Yu, P. Guan, Y. Wang, and Y. Zhao, "Spatial spectrum-based channel estimation for wideband mmWave system with beam squint," *IEEE Access*, vol. 9, pp. 16 164–16 172, 2021.

[17] J. Zhao, J. Liu, F. Gao, W. Jia, and W. Zhang, "Gridless compressed sensing based channel estimation for UAV wideband communications with beam squint," *IEEE Transactions on Vehicular Technology*, vol. 70, no. 10, pp. 10 265–10 277, 2021.

[18] J.-F. Cai, E. J. Candés, and Z. Shen, "A singular value thresholding algorithm for matrix completion," *SIAM Journal on Optimization*, vol. 20, no. 4, pp. 1956–1982, 2010.